INORGANIC CHEMISTRY
FRONTIERS

RESEARCH ARTICLE

View Article Online
View Journal | View Issue

Cite this: *Inorg. Chem. Front.*, 2019, **6**, 1081

Hyperfine coupling and slow magnetic relaxation in isotopically enriched Dy^{III} mononuclear single-molecule magnets†

Jessica Flores Gonzalez, Fabrice Pointillart * and Olivier Cador *

Received 7th November 2018,
Accepted 31st January 2019

DOI: 10.1039/c8qi01209a

rsc.li/frontiers-inorganic

The four main stable isotopes of the $[^{A}Dy(tta)_3(\mathbf{L})]\cdot C_6H_{14}$ (**^{A}Dy** with A = 161–164) Single-Molecule Magnet (SMM) (tta^- = 2-thenoyltrifluoroacetylacetonate and **L** = 2-{[2-methylpyridiyl]-4,5-[4,5-bis(propylthio)-tetrathiafulvalenyl]-1*H*-benzimidazol-2-yl}pyridine) have been magnetically investigated and structurally characterized by single crystal X-ray diffraction. The two nuclear spin-free **$^{162/164}$Dy** behave the same from a dynamic magnetic point of view and with slower magnetic relaxation than the two pure magnetically active isotopically substituted **$^{161/163}$Dy**. In addition, this paper demonstrates that **^{161}Dy** and **^{163}Dy** relax differently even if they both carry I = 5/2 nuclear spin. After the release of the dipolar interactions through magnetic dilution, ($[^{161}Dy_{0.05}Y_{0.95}(tta)_3(\mathbf{L})]\cdot C_6H_{14}$) (**^{161}Dy@Y**) relaxes four times slower than **^{163}Dy@Y** due to different hyperfine coupling constants.

Introduction

The possibility to observe a magnetic memory at the single-ion level for a lanthanide ion was demonstrated in 2003 for a $[TbPc_2]$ (Pc = phthalocyaninato) complex.[1,2] Since that discovery, lanthanide-based mononuclear Single-Molecule Magnets (SMMs) have been designed for their potential applications in high-density data storage[3] and spintronic devices.[4]

On one hand, the integration of lanthanide SMMs in devices for data storage is limited due to the low-temperature range at which such molecular systems highlight magnetic memory. To overcome such a limitation, few strategies have been explored: (i) a molecular engineering strategy to induce an adequate symmetry and crystal field around the lanthanide ion leading to an optimal crystal splitting of the ground multiplet state. Such a strategy has recently driven chemists to design a hexa-*tert*-butyldysprosocenium complex with an exceptional magnetic axiality and a blocking temperature of 60 K;[5,6,7–10] (ii) the minimization of the magnetic moment perturbation by magnetic dilution by adding the complex to a frozen solution[11] or doping it with a diamagnetic isomorphous matrix[12] which leads to the isolation of the electronic spin carriers; and (iii) the minimization of the hyperfine interactions by isotopic enrichment in nuclear spin-free lanthanides which leads to a diminution of the Quantum Tunnelling of Magnetization (QTM) efficiency.[13,14]

On the other hand, lanthanide SMMs could be suitable to perform nuclear spin qubits/qudits[4,15–18] due to the several DiVincenzo characteristics[19,20] already observed for such systems. In other words, two nuclear isomers of a lanthanide SMM could be used to enhance the magnetic performance for data storage (nuclear spin-free isomer) while the pure nuclear spin isomer could be used as a multilevel nuclear spin qubit (qudit) because of the nuclear-spin-driven QTM events.[21] Nevertheless the Dy^{III} ion is composed of seven isotopes with nuclear spin values of 0 and 5/2. The four main ^{161}Dy, ^{162}Dy, ^{163}Dy and ^{164}Dy isotopes represent 97.5% of the isotopic mixture but until now only two of them have been studied on the same system.[13,14,21]

In this paper, we propose to go a step further in studying four stable isotopically enriched dysprosium complexes ($[^{A}Dy(tta)_3(\mathbf{L})]\cdot C_6H_{14}$ [22] where tta^- = 2-thenoyltrifluoroacetylacetonate, **L** = 2-{[2-methylpyridiyl]-4,5-[4,5-bis(propylthio)-tetrathiafulvalenyl]-1*H*-benzimidazol-2-yl}pyridine) and A = 161, 162, 163 and 164 (abbreviated as **^{A}Dy** here after). It is worth noting that **^{161}Dy** and **^{164}Dy** have been previously studied by some of us.[13] The aim of this study was to pursue the investigations on an identical system for which all the synthetic steps are under control. The two ^{161}Dy and ^{163}Dy isotopes possess the same nuclear spin value (I = 5/2) but not the same nuclear magnetic moment while the ^{162}Dy and ^{164}Dy isotopes possess no nuclear spins. Magnetic dilution of the dysprosium complexes in an isomorphous diamagnetic matrix based on yttrium (**^{A}Dy@Y**) has been systematically performed to cancel dipolar interactions in the condensed phase.

Univ Rennes, CNRS, ISCR (Institut des Sciences Chimiques de Rennes) - UMR 6226, F-35000 Rennes, France. E-mail: olivier.cador@univ-rennes1.fr

†Electronic supplementary information (ESI) available. See DOI: 10.1039/c8qi01209a

Materials and methods

The elemental analyses of the compounds were performed at the Centre Régional de Mesures Physiques de l'Ouest, Rennes. The Dy/Y ratio of the compounds **^{162}Dy@Y** and **^{163}Dy@Y** was determined using SEM (Scanning Electron Microscopy). All observations and measurements were carried out with a JEOL JSM 6400 scanning electron microscope (JEOL Ltd, Tokyo, Japan) with an EDS (Energy Dispersive Spectrometry) analysis system (Oxford Link INCA). The voltage was kept at 9 kV, and the samples were mounted on carbon stubs and coated for 5 min with a gold/palladium alloy using a sputter coater (Jeol JFC 1100). This analysis has been performed by the "Centre de Microscopie Electronique à Balayage et microAnalyse (CMEBA)" from the University of Rennes 1 (France). The dc magnetic susceptibility measurements were performed on solid polycrystalline samples with a Quantum Design MPMS-XL SQUID magnetometer between 2 and 300 K in an applied magnetic field of 200 Oe for temperatures between 2 and 20 K, 2 kOe between 20 and 80 K and 10 kOe above 80 K. Making measurements at various applied fields allows us to verify that the samples are free from ferromagnetic impurities and also avoid saturation phenomena at low temperature. These measurements were all corrected for the diamagnetic contribution as calculated with Pascal's constants.

Experimental

All solvents were dried using standard procedures. 4,5-Bis(propylthio)-tetrathiafulvalene-2-(2-pyridyl)benzimidazole-methyl-2-pyridine ligand (**L**) was synthesized following a published procedure.[23] The isotopically enriched Dy_2O_3 oxides are commercially available from Eurisotop company. All other reagents were purchased from Aldrich Co. Ltd and were used without further purification.

Isotopically enriched $Dy(tta)_3{\cdot}2H_2O$ compounds are prepared according to the following modified literature procedure:[24] on one side, 47.1 mg (0.126 mmol) of Dy_2O_3 enriched at 94.4% in $^{162}Dy^{III}$ or at 95.0% in $^{163}Dy^{III}$ were placed in the presence of 130 μL of concentrated HCl. After 30 min of stirring at 50 °C, the resulting solution of $^{162/163}DyCl_3{\cdot}6H_2O$ was diluted with 1 mL of water. On the other side, 224 mg of Htta (1.010 mmol) were dissolved in 180 mL of water at 60 °C under intense stirring. The pH of the solution was adjusted to 6–6.5 with NH_4OH. To the obtained solution was added an aqueous solution of isotopically enriched $DyCl_3{\cdot}6H_2O$ (0.252 mmol). The pH of the solution was adjusted to 7–7.5 during the stirring and then flocculation of $Dy(tta)_3{\cdot}2H_2O$ took place and was filtered. Yield $^{162}Dy(tta)_3{\cdot}2H_2O$: 115 mg (53%). Yield $^{163}Dy(tta)_3{\cdot}2H_2O$: 110 mg (51%).

$[^{162/163}Dy(tta)_3(\mathbf{L})]{\cdot}C_6H_{14}$ (**^{162}Dy** and **^{163}Dy**): a CH_2Cl_2 solution of **L** (24.4 mg, 0.04 mmol) and $^{162/163}Dy(tta)_3{\cdot}2H_2O$ (34.5 mg, 0.04 mmol) is stirred for 1 hour. *n*-Hexane is layered to the solution and red prismatic single crystals are obtained after two weeks of diffusion and evaporation at room temperature. Yield **^{162}Dy**: 47.7 mg (83%). Yield **^{163}Dy**: 50.0 mg (87%). Anal. calcd (%) for $C_{52}H_{38}DyF_9N_4O_6S_9$: C 43.47, H 2.65, N 3.90; found **^{162}Dy**: C 43.61, H 2.72, N 3.79. found **^{163}Dy**: C 43.66, H 2.77, N 3.83.

$[^{162/163}Dy_{0.05}Y_{0.95}(tta)_3(\mathbf{L})]{\cdot}C_6H_{14}$ (**$^{162/163}$Dy@Y**): a CH_2Cl_2 solution (15 mL) of **L** (61.0 mg, 0.1 mmol) is added to a CH_2Cl_2 solution (10 mL) containing $^{162/163}Dy(tta)_3{\cdot}2H_2O$ (3.4 mg, 0.004 mmol) and $Y(tta)_3{\cdot}2H_2O$ (75.7 mg, 0.096 mmol) and stirred for 1 hour. *n*-Hexane is layered to the solution and red prismatic single crystals are obtained after two weeks of diffusion and evaporation at room temperature. Yield **^{162}Dy@Y**: 47.7 mg (80%). Yield **^{163}Dy@Y**: 50.0 mg (85%). $C_{52}H_{38}Dy_{0.05}Y_{0.95}F_9N_4O_6S_9$: C 45.69, H 2.78, N 4.10; found **^{162}Dy**: C 45.60, H 2.82, N 3.99; found **^{163}Dy**: C 45.66, H 2.87, N 4.03.

Results and discussion

Structural description

The four compounds **^{162}Dy**, **^{163}Dy**, **^{162}Dy@Y** and **^{163}Dy@Y** are isostructural (Table S1, Fig. S1–S4†). The ratio Dy/Y (0.05/0.95) for the two doped compounds $[^{162}Dy_{0.05}Y_{0.95}(tta)_3(\mathbf{L})]{\cdot}C_6H_{14}$ (**^{162}Dy@Y**) and $[^{163}Dy_{0.05}Y_{0.95}(tta)_3(\mathbf{L})]{\cdot}C_6H_{14}$ (**^{163}Dy@Y**) has been determined by EDS analysis and then it is used to refine the X-ray structure on single crystals. The X-ray structures for the natural isotopes, **^{161}Dy** and **^{164}Dy**, have been studied in our previous work.[13,22] Thus a single and rapid structural description is given below to understand the structural characteristic of the system.

The X-ray structures consist of a mononuclear complex of Dy^{III} which lies in a N_2O_6 coordination environment with a square antiprism symmetry. Three tta^- anions and the ligand **L** provide the six oxygen and two nitrogen atoms, respectively (Fig. 1). As expected, the Dy–N bond length is longer than the Dy–O ones due to the oxophilic character of the lanthanide. The central C=C bond length and the non-planar TTF core confirm the neutrality of **L**. The crystal packing highlighted the formation of "head-to-tail" dimers of complexes (Fig. S5†).

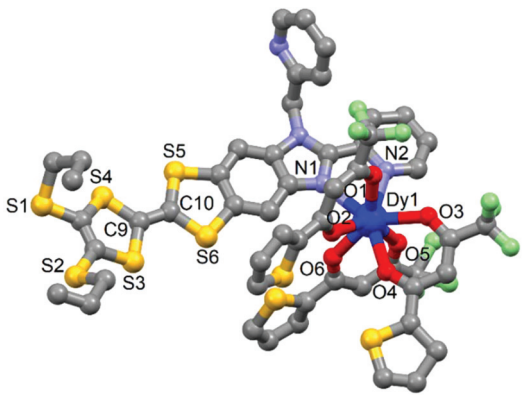

Fig. 1 Molecular structure of **^{163}Dy**. Hydrogen atoms and CH_2Cl_2 molecule of crystallization are omitted for clarity.

Static magnetic properties

The thermal dependence of the magnetic susceptibility and the first magnetization at 2 K are measured for the **^{162}Dy** and **^{163}Dy** samples and for **^{162}Dy@Y** and **^{163}Dy@Y** (Fig. S6 and S7†). The $\chi_M T$ *vs.* T and M *vs.* H curves are identical for the two isotopes because the static magnetic properties are independent of the nuclear magnetic moment. The experimental values are in agreement with the expected values for a single Dy^{III} ion.[25]

Dynamic magnetic properties

The dynamic magnetic properties of the two isotopologues **^{162}Dy** (I = 0) and **^{163}Dy** (I = 5/2) are determined by measuring the frequency dependences of the magnetic susceptibility (Fig. 2, S9 and S10†). Both isotopologues display a frequency dependence for the out-of-phase component, χ_M'', of the ac susceptibility in a zero external dc field, a sign of slow magnetic relaxation. As previously observed for **^{161}Dy** and **^{164}Dy**, the maximum on the χ_M'' *vs.* ν curve (where ν is the frequency of the oscillating field) occurs at a lower frequency for the nuclear spin-free isotope (16 Hz) than for the isotope with I = 5/2 (160 Hz).

The relaxation times (τ) for both isotopologues have been extracted with an extended Debye model (see the ESI†). Their temperature dependences follow a modified Arrhenius law ($\tau^{-1} = \tau_0^{-1} \exp(\Delta/T) + \tau_{TI}^{-1}$) (where τ_0 and τ_{TI} are, respectively, the intrinsic and temperature-independent relaxation times and Δ is the energy barrier) (Fig. 3, Tables 1, S2 and S3†). Both Δ and τ_0 remain almost identical for **^{162}Dy** and **^{163}Dy**, suggesting that the thermally activated regime is not affected by the nucleus and thus by the hyperfine interactions (Table 1, Fig. S11 and S12†), while the thermally independent regime (QTM) is strongly affected by the isotopic enrichment with the cancellation of the nuclear spin of dysprosium (Fig. 3). Even if the QTM is reduced, it is still operative at a low temperature. To cancel this, an optimal magnetic field of 1000 Oe is applied (Fig. S13–S16†), leading to a drastic slowing down of the magnetic relaxation. Nevertheless, such an intense magnetic field also cancels the isotopic effect. In fact the two Arrhenius plots for both **^{162}Dy** and **^{163}Dy** are superimposed (Fig. S17†). Fig. 3 provides an easy comparison between all isotopologues. As expected, the two nuclear spin-free isotopes **^{162}Dy** and **^{164}Dy** behave the same whereas the two isotopes **^{161}Dy** and **^{163}Dy** (I = 5/2) display faster magnetic relaxation. In the QTM regime, a significant difference exists between **^{161}Dy** and **^{163}Dy**. Fig. 4 shows the χ_M'' *vs.* ν curves for the two **^{161}Dy** and **^{163}Dy** with respective maxima centred at 106 Hz and 160 Hz, respectively. **^{163}Dy** relaxes slightly faster than **^{161}Dy**. This can be compared with the very different (of opposite sign) hyperfine coupling constants of ^{161}Dy and ^{163}Dy.[26] Furthermore, the hyperfine interactions are expected to be stronger for the isotope **^{163}Dy** than for **^{161}Dy**,[27] leading to a more efficient QTM for the former as experimentally observed (Fig. 3 and Table 1). The effect of the nuclear spin value and, *a fortiori*, the effect of the hyperfine constant value are very sensitive to any magnetic field (external or internal) because the hyperfine interaction, of the order of a few thousandths of wavenumber, is easily destroyed by the dipolar magnetic field generated by intermolecular interactions. In order to evaluate the exact effect of the hyperfine coupling constants for the two **^{161}Dy** and **^{163}Dy** isotopes, the internal magnetic field has been released in the doped samples $[^{161}Dy_{0.03}Y_{0.97}(tta)_3(\mathbf{L})]\cdot C_6H_{14}$ (**^{161}Dy@Y**, the data come from our previous work[13]) and $[^{163}Dy_{0.05}Y_{0.95}(tta)_3(\mathbf{L})]\cdot C_6H_{14}$ **^{163}Dy@Y**. The frequency dependences, in the zero external field, of the two doped isotopolo-

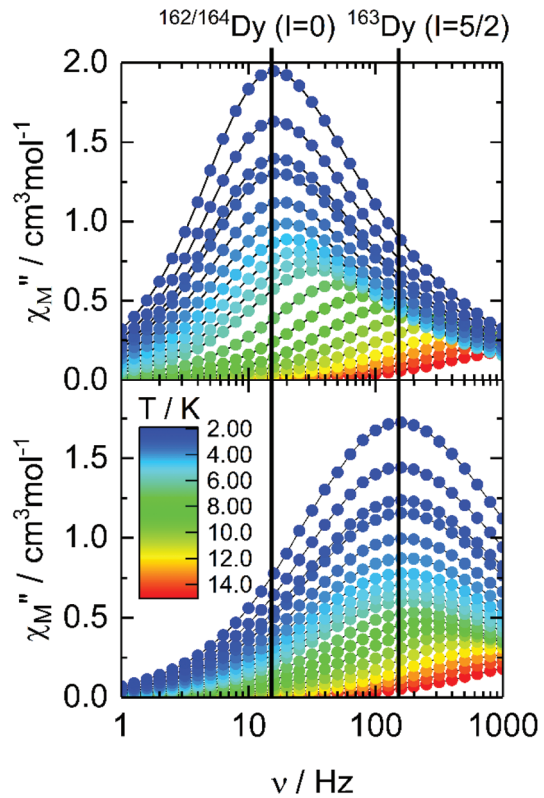

Fig. 2 Frequency dependences of χ_M'' of **^{162}Dy** and **^{163}Dy** in a zero magnetic field in the temperature range of 2–15 K.

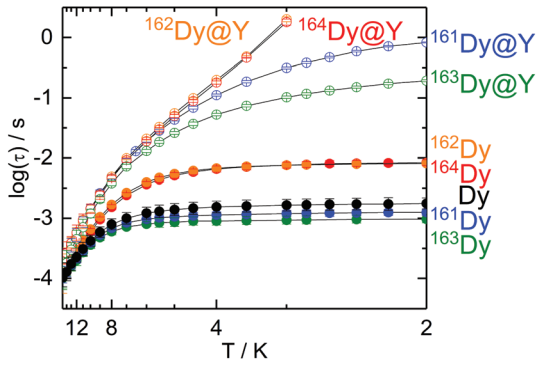

Fig. 3 Temperature dependences of the relaxation times τ of the four main stable isotopologues **$^{161-164}$Dy** (full circles) and diluted samples **$^{161-164}$Dy@Y** in a zero magnetic field in the temperature range of 2–15 K. Full lines are guides to the eye only.

Table 1 Dynamic parameters of the four, pure and diluted, isotopologues of **Dy**

	Dy	**^{161}Dy** $I = 5/2$	**^{162}Dy** $I = 0$	**^{163}Dy** $I = 5/2$	**^{164}Dy** $I = 0$
Δ/K	43	45	44	46	43
τ_0/s	$6.7(1) \times 10^{-6}$	$6.0(8) \times 10^{-6}$	$7.8(1) \times 10^{-6}$	$5.6(7) \times 10^{-6}$	$7.7(9) \times 10^{-6}$
τ_{TI}/s[a]	$1.8(1) \times 10^{-3}$	$1.3(1) \times 10^{-3}$	$8.1(1) \times 10^{-3}$	$1.0(1) \times 10^{-3}$	$8.3(1) \times 10^{-3}$
	Dy@Y	**^{161}Dy@Y**	**^{162}Dy@Y**	**^{163}Dy@Y**	**^{164}Dy@Y**
Δ/K	Not measured	58	59	57	60
τ_0/s		$4.0(10) \times 10^{-6}$	$3.5(9) \times 10^{-6}$	$3.9(6) \times 10^{-6}$	$3.8(8) \times 10^{-6}$
τ_{TI}/s[a]		0.83(6)	$\approx 100^{b}$	0.19(0.4)	$\approx 100^{b}$

[a] Values extracted from the experimental data at 2 K. [b] Values obtained by extrapolation of the experimental data.

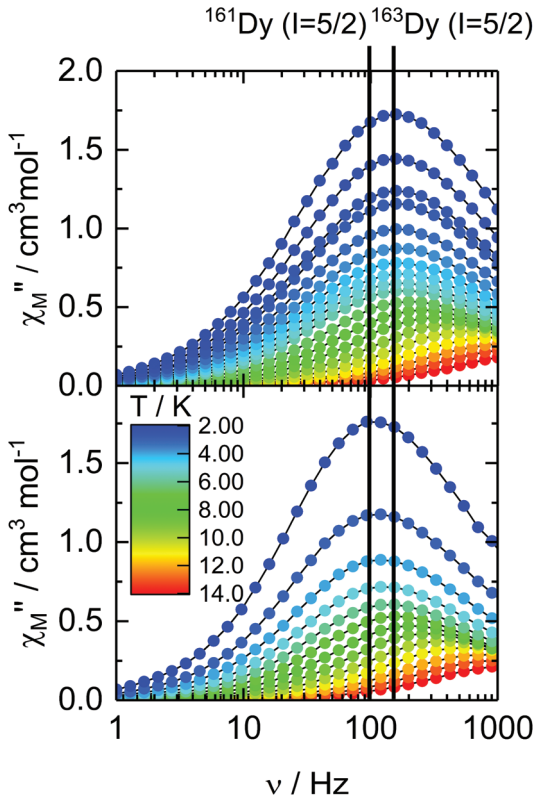

Fig. 4 Frequency dependences of χ_M'' of **^{161}Dy** and **^{163}Dy** in a zero magnetic field in the temperature range of 2–14 K.

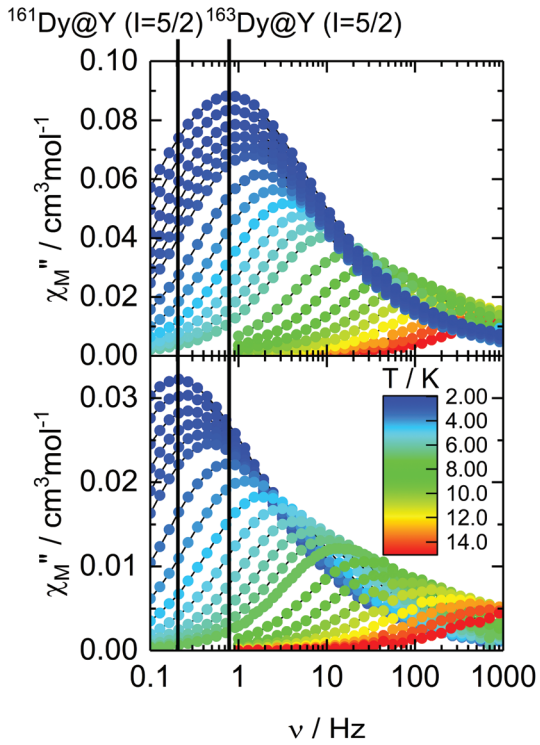

Fig. 5 Frequency dependences of χ_M'' of **^{161}Dy@Y** and **^{163}Dy@Y** in a zero magnetic field in the temperature range of 2–15 K.

gues are depicted in Fig. 5 and S18–S21.† The cancelling of the internal magnetic field has two consequences on the magnetic properties of the doped samples: (1) the maxima of the out-of-phase component of the magnetic susceptibility are shifted to lower frequencies for both **^{161}Dy@Y** (0.2 Hz) and **^{163}Dy@Y** (0.8 Hz) with respect to the condensed phase (Fig. 3 and Tables 1, S7†). This is even true at the lowest temperatures where the relaxation time becomes almost 1000 times slower than that in the condensed phase. (2) The difference between the two doped isotopologues (**^{161}Dy@Y** and **^{163}Dy@Y**) is much more pronounced, with, at 2 K, the relaxation time of **^{161}Dy@Y** being four times slower than that of **^{163}Dy@Y**. Considering that the magnetic entities in **^{161}Dy@Y** and **^{163}Dy@Y** are perfectly isolated systems, the difference observed is entirely due to hyperfine coupling. As expected, the relaxation tends to become thermally independent at low temperature. Therefore, a hyperfine coupling effect on the magnetic relaxation of a molecule can only be probed in diluted systems. Of course, the release of the hyperfine coupling in nuclear spin-free systems such as **^{162}Dy@Y** and **^{164}Dy@Y** produces slower relaxation (Fig. 3 and Table S6†) which never ends in a thermally independent regime at low temperature. At this stage, relaxation is governed by Orbach or Raman processes or a combination of these two processes.

The hysteresis loops for **^{161}Dy@Y** and **^{163}Dy@Y** were compared and classical butterfly shaped hysteresis loops for the

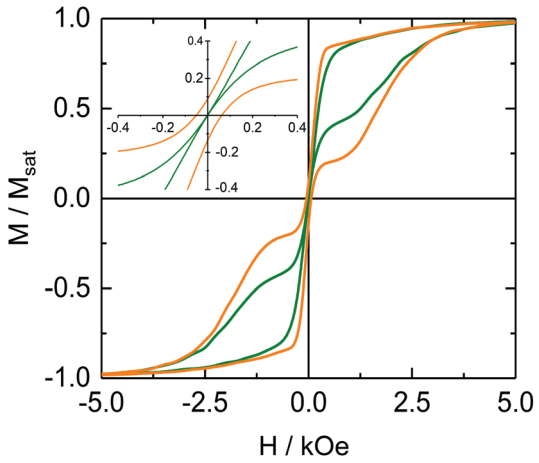

Fig. 6 Normalized magnetic hysteresis loops at 0.48 K and at a sweep rate of 16 Oe s^{-1} for ^{162}**Dy@Y** (orange lines) and ^{163}**Dy@Y** (green lines). The inset is a zoomed view of the origin to visualize the remnant magnetization.

Dy^{III} mononuclear SMM are observed but no significant differences are observed between the two isotopes (Fig. S22†), whereas the hysteresis loops of the doped compounds with the fastest (^{163}**Dy@Y**) and the slowest (^{162}**Dy@Y** or ^{164}**Dy@Y**) relaxation of magnetization show significant differences with a clear magnetic bistability at a zero-magnetic field for the nuclear spin-free ^{162}**Dy@Y** (Fig. 6). In contrast, ^{163}**Dy@Y** is closed at zero field in agreement with the relaxation measurements.

Conclusions

The two 162 and 163 isotopes of the Dy^{III} mononuclear Single-Molecule Magnet $[Dy(tta)_3(\mathbf{L})]\cdot C_6H_{14}$ were investigated and then compared with the two 161 and 164 isotopes previously studied by some of us. The nuclear spin-free isotope (^{162}**Dy**) displayed a slower magnetic relaxation in the thermally independent regime compared to the isotope ^{163}**Dy** (I = 5/2) due to the cancelling of the hyperfine interactions coming from the metal centre. As expected, the two nuclear spin-free ^{162}**Dy** and ^{164}**Dy** behaved as the same while a significant difference of the relaxation time of magnetization was observed between the two ^{161}**Dy** and ^{163}**Dy** isotopic isomers (I = 5/2). At 2 K, the ^{163}**Dy** isotope relaxed 50% faster than ^{161}**Dy** because of the greater hyperfine interaction constants for the former compared to the latter. Finally after removing the dipolar magnetic interactions by doping, the effect of the hyperfine interaction constants on magnetic relaxation is directly observed with ^{163}**Dy@Y** which relaxed 300% faster than ^{161}**Dy@Y**.

Future Dy^{III} isotopic enrichment in which Dy^{III} is in a nuclear spin-free environment is under investigation in order to determine the effect of the hyperfine coupling arising from the first neighbouring atoms and the effect of the oblate *versus* prolate electronic distribution of the lanthanide ion.

Conflicts of interest

There are no conflicts to declare.

Acknowledgements

This work was supported by the CNRS, Université de Rennes and the European Research Council through the ERC-CoG 725184 MULTIPROSMM (project no. 725184).

Notes and references

1 R. Giraud, W. Wernsdorfer, A. M. Tkachuk, D. Mailly and B. Barbara, *Phys. Rev. Lett.*, 2001, **87**, 057203.
2 N. Ishikawa, M. Sugita, T. Ishikawa, S. Koshihara and Y. Kaizu, *J. Am. Chem. Soc.*, 2003, **125**, 8694–8695.
3 D. Gatteschi, R. Sessoli and J. Villain, *Molecular Nanomagnets*, Oxford University Press, 2006.
4 S. Thiele, F. Balestro, R. Ballou, S. Klyatskaya, M. Ruben and W. Wernsdorfer, *Science*, 2014, **344**, 1135–1138.
5 F.-S. Guo, B. M. Day, Y.-C. Chen, M.-L. Tong, A. Mansikkamäki and R. A. Layfield, *Angew. Chem., Int. Ed.*, 2017, **56**, 11445–11449.
6 C. A. P. Goodwin, F. Ortu, D. Reta, N. F. Chilton and D. P. Mills, *Nature*, 2017, **548**, 439–442.
7 F.-S. Guo, B. M. Day, Y.-C. Chen, M.-L. Tong, A. Mansikkamäki and R. A. Layfield, *Science*, 2018, eaav0652.
8 L. Ungur, S.-Y. Lin, J. Tang and L. F. Chibotaru, *Chem. Soc. Rev.*, 2014, **43**, 6894–6905.
9 Z. Zhu, M. Guo, X.-L. Li and J. Tang, *Coord. Chem. Rev.*, 2019, **378**, 350–364.
10 P. Zhang, Y.-N. Guo and J. Tang, *Coord. Chem. Rev.*, 2013, **257**, 1728–1763.
11 G. Cosquer, F. Pointillart, S. Golhen, O. Cador and L. Ouahab, *Chem. – Eur. J.*, 2013, **19**, 7895–7903.
12 F. Habib, P. H. Lin, J. Long, I. Korobkov, W. Wernsdorfer and M. Murugesu, *J. Am. Chem. Soc.*, 2011, **133**, 8830–8833.
13 F. Pointillart, K. Bernot, S. Golhen, B. Le Guennic, T. Guizouarn, L. Ouahab and O. Cador, *Angew. Chem., Int. Ed.*, 2015, **54**, 1504–1507.
14 Y. Kishi, F. Pointillart, B. Lefeuvre, F. Riobé, B. Le Guennic, S. Golhen, O. Cador, O. Maury, H. Fujiwara and L. Ouahab, *Chem. Commun.*, 2017, **53**, 3575–3578.
15 S. Thiele, R. Vincent, M. Holzmann, S. Klyatskaya, M. Ruben, F. Balestro and W. Wernsdorfer, *Phys. Rev. Lett.*, 2013, **111**, 037203.
16 R. Vincent, *Nature*, 2012, **488**, 357–360.
17 D. P. O'Leary, G. K. Brennen and S. S. Bullock, *Phys. Rev. A*, 2006, **74**, 032334.
18 M. Leuenberger and D. Loss, *Nature*, 2001, **410**, 789–793.

19 K. S. Pedersen, A.-M. Ariciu, S. McAdams, H. Weihe, J. Bendix, F. Tuna and S. Piligkos, *J. Am. Chem. Soc.*, 2016, **138**, 5801–5804.
20 D. Aguilà, L. A. Barrios, V. Velasco, O. Roubeau, A. Repollés, P. J. Alonso, J. Sesé, S. J. Teat, F. Luis and G. Aromí, *J. Am. Chem. Soc.*, 2014, **136**, 14215–14222.
21 E. Moreno-Pineda, M. Damjanović, O. Fuhr, W. Wernsdorfer and M. Ruben, *Angew. Chem., Int. Ed.*, 2017, **56**, 9915–9919.
22 T. T. da Cunha, J. Jung, M.-E. Boulon, G. Campo, F. Pointillart, C. L. M. Pereira, B. Le Guennic, O. Cador, K. Bernot, F. Pineider, S. Golhen and L. Ouahab, *J. Am. Chem. Soc.*, 2013, **135**, 16332–16335.
23 G. Cosquer, F. Pointillart, J. Jung, B. Le Guennic, S. Golhen, O. Cador, Y. Guyot, A. Brenier, O. Maury and L. Ouahab, *Eur. J. Inorg. Chem.*, 2014, **2014**, 69–82.
24 A. I. Voloshin, N. Shavaleev and V. P. Kazakov, *J. Lumin.*, 2000, **91**, 49–58.
25 O. Kahn, *Molecular magnetism*, VCH, 1993.
26 W. Ebenhöh, V. J. Ehlers and J. Ferch, *Z. Phys.*, 1967, **200**, 84–92.
27 W. J. Childs, *Phys. Rev. A*, 1970, **2**, 1692–1701.

